

cHyRRT and cHySST: Two Motion Planning Tools for Hybrid Dynamical Systems

Beverly Xu, Nan Wang, Ricardo G. Sanfelice

xu21beve@gmail.com, nanwang@ucsc.edu, ricardo@ucsc.edu

November 19, 2024

Technical Report
Hybrid Systems Laboratory
Department of Computer Engineering
University of California, Santa Cruz

Technical Report No. TR-HSL-10-2024

Available at <https://hybrid.soe.ucsc.edu/biblio>

Readers of this material have the responsibility to inform all of the authors promptly if they wish to reuse, modify, correct, publish, or distribute any portion of this report.

Abstract

This paper describes two C++/Open Motion Planning Library implementations of the recently developed motion planning algorithms HyRRT Wang and Sanfelice [2022] and HySST Wang and Sanfelice [2023]. Specifically, cHyRRT, an implementation of the HyRRT algorithm, is capable of generating a solution to a motion planning problem for hybrid systems with probabilistically completeness, while cHySST, an implementation of the asymptotically near-optimal HySST algorithm, is capable of computing a trajectory to solve the optimal motion planning problem for hybrid systems. cHyRRT is suitable for motion planning problems where an optimal solution is not required, whereas cHySST is suitable for such problems that prefer optimal solutions, within all feasible solutions. The structure, components, and usage of the two tools are described. Examples are included to illustrate the main capabilities of the toolbox.

Keywords: Motion Planning; Hybrid Systems; Rapidly-exploring Random Trees; Stable-sparse RRT

1 Introduction

Motion planning is becoming an increasingly important tool for researchers and practitioners as robotic systems enter operation in more complex environments, such as in narrow, indoor spaces Lopes et al. [2016] and in traffic Yang et al. [2022], and with increasingly complex dynamics, such as in quadrupled robots Biswal and Mohanty [2021], manipulators Piazza et al. [2019], and drones Ahmed et al. [2022]. Significant progress has been made in the implementation of motion planners for high-dimensional systems in the widely-used Open Motion Planning Library (OMPL) Sukan et al. [2012]. Several recent additions to the sampling-based motion planning library include Advanced BIT* Strub and Gammell [2020], Space-time RRT* Grothe et al. [2022], and Task-space RRT Luna et al. [2020]. Such implementations are examples of well-developed motion planning algorithms for purely continuous-time systems and purely discrete-time systems. However, motion planning for hybrid systems, in which the states can evolve continuously and, at times, exhibit jumps, along with implementations of such algorithms, are still open problems.

We consider the hybrid equation framework where a hybrid dynamical system is given by Goebel et al. [2009]:

$$\mathcal{H} : \begin{cases} \dot{x} = f(x, u) & (x, u) \in C \\ x^+ = g(x, u) & (x, u) \in D \end{cases} \quad (1)$$

where $x \in \mathbb{R}^n$ is the state, $u \in \mathbb{R}^m$ is the input, $C \subset \mathbb{R}^n \times \mathbb{R}^m$ represents the flow set, $f : \mathbb{R}^n \times \mathbb{R}^m \rightarrow \mathbb{R}^n$ represents the flow map, $D \subset \mathbb{R}^n \times \mathbb{R}^m$ represents the jump set, and $g : \mathbb{R}^n \times \mathbb{R}^m \rightarrow \mathbb{R}^n$ represents the jump map. The continuous evolution of x is captured by the flow map f . The discrete evolution of x is captured by the jump map g . The flow set C collects the

points where the state can evolve continuously. The jump set D collects the points where jumps can occur. In this modeling framework, differential and difference equations with constraints are used to describe the continuous and discrete behavior of the hybrid system, respectively; see Goebel et al. [2009] for a detailed definition. This general hybrid system framework can capture most hybrid systems emerging in robotic applications, not only the class of hybrid systems considered in Branicky et al. [2003], but also systems with timers, impulses, and constraints.

Within this framework, we present two tools for motion planning. Rapidly-exploring Random Trees (RRT), in practice, as a sampling-based algorithm, is able to compute trajectories for high-dimension systems more efficiently by incrementally constructing a search tree through randomly sampling the state space. Following the RRT algorithm scheme, HyRRT in Wang and Sanfelice [2022] is proposed to solve the motion planning problem for hybrid systems, inheriting its computation advantages while addressing hybrid systems, which is general to capture purely continuous-time and purely discrete-time systems as well. A key advantage of HyRRT is that, as an RRT-type algorithm, it is probabilistically complete, meaning the probability of failing to find a motion plan converges to zero as the number of samples approaches infinity LaValle [1998]. At each iteration, HyRRT randomly picks a state sample and extends the search tree by flow or jump, which is also chosen randomly when both regimes are possible. Therefore, the planner takes in flow and jump maps f and g and flow and jump sets C and D representing the system’s dynamics, starting, final, and unsafe state sets, to return an OMPL solution status and OMPL motion plan.

In many motion planning applications, an optimal solution is desired over a feasible, sub-optimal one Yang [2019]. Solutions generated by RRT converge to a sub-optimal solution Nechushtan et al. [2010], while variants of Probabilistic Road Map and RRT, such as PRM* and RRT* Karaman and Frazzoli [2011], which solve optimal motion planning problems with guaranteed asymptotic optimality, require a steering function that limits their application. On the other hand, the stable sparse RRT (SST) algorithm presented in Li et al. [2016] does not require a steering function and is guaranteed to be asymptotically near optimal, which means that the probability of finding a solution that has a cost close to the minimal cost converges to one as the number of iterations goes to infinity. A key advantage of HySST over HyRRT is that, as an SST-type algorithm, HySST generates near-optimal solutions. HySST differs from HyRRT in two aspects: i) HySST takes in the input pruning radius $\delta_S \in \mathbb{R}_{>0}$ to remove all vertices, excluding the vertex with the lowest cost, within δ_S of the static, witness state, and ii) HySST takes in the input selection radius $\delta_{BN} \in \mathbb{R}_{>0}$ to select the vertex with the lowest cost within δ_{BN} of the randomly sampled vertex to start propagation from. If there are no vertices within the ball defined by radius δ_{BN} , then the nearest vertex is selected.

To date, there are no such implementations of motion planners for hybrid dynamical systems in OMPL Şucan et al. [2012]. Such planners are highly valuable because OMPL not only contains tools for benchmarking, but is also

compatible with the widely used Robot Operating System (ROS) Macenski et al. [2022], both directly and through the most widely-used robotic manipulation software: MoveIt 2¹, which is also the core ROS 2 robotics manipulation platform. Compatibility with ROS, which contains libraries and tools for developing, simulating, and visualizing robots, is a notable advantage of both tools. To generate a motion plan for a given hybrid systems, we introduce cHyRRT and cHySST. Both tools consist of functions to define the hybrid system and simulate dynamics, set-checking functions to satisfy both state-space safety and kinodynamic constraints, and a script to visualize the generated trajectories in the ROS 2 visualization package RViz 2.

The remainder of the paper is structured as follows. Section 2 presents notation and preliminaries. Section 3 presents the motion planning problem for hybrid dynamical systems. Section 4 presents the HyRRT algorithm and details of cHyRRT’s implementation, usage, and customizations. Section 5 presents the HySST algorithm, including details of cHySST’s implementation, usage, and customizations. Section 6 presents example applications of both algorithms and illustrations of the generated motion plans. Next, we will describe notation and preliminaries used throughout this paper.

2 Notation and Preliminaries

2.1 Notation

In this paper, the set of real numbers is denoted as \mathbb{R} and its nonnegative subset is denoted as $\mathbb{R}_{\geq 0}$. The set of nonnegative integers is denoted as \mathbb{N} . The notation $\text{int } I$ denotes the interior of the interval I . Given sets $P \subseteq \mathbb{R}^n$ and $Q \subseteq \mathbb{R}^n$, the Minkowski sum of P and Q , denoted as $P + Q$, is the set $\{p + q : p \in P, q \in Q\}$. The notation $\text{rge } f$ denotes the range of the function f .

2.2 Preliminaries

Given a flow set C , the set $U_C := \{u \in \mathbb{R}^m : \exists x \in \mathbb{R}^n \text{ such that } (x, u) \in C\}$ includes all possible input values that can be applied during flows. Similarly, given a jump set D , the set $U_D := \{u \in \mathbb{R}^m : \exists x \in \mathbb{R}^n \text{ such that } (x, u) \in D\}$ includes all possible input values that can be applied at jumps. These sets satisfy $C \subseteq \mathbb{R}^n \times U_C$ and $D \subseteq \mathbb{R}^n \times U_D$. Given a set $K \subseteq \mathbb{R}^n \times U_\star$, where \star is either C or D , we define $\pi_\star(K) := \{x : \exists u \in U_\star \text{ such that } (x, u) \in K\}$ as the projection of K onto \mathbb{R}^n , and define $C := \pi_C(C)$ and $D := \pi_D(D)$.

In addition to ordinary time $t \in \mathbb{R}_{\geq 0}$, we employ $j \in \mathbb{N}$ to denote the number of jumps of the evolution of x and u for \mathcal{H} in (1), leading to hybrid time (t, j) for the parameterization of its solutions and inputs. The domain of a solution to \mathcal{H} is given by a hybrid time domain. A hybrid time domain is defined as a subset E of $\mathbb{R}_{\geq 0} \times \mathbb{N}$ that, for each $(T, J) \in E$, $E \cap ([0, T] \times \{0, 1, \dots, J\})$ can be written as $\bigcup_{j=0}^J ([t_j, t_{j+1}], j)$ for some finite sequence of times $0 = t_0 \leq t_1 \leq$

¹See <https://moveit.ai/> for more information about the MoveIt library

$t_2 \leq \dots \leq t_{J+1} = T$. A hybrid arc $\phi : \text{dom } \phi \rightarrow \mathbb{R}^n$ is a function on a hybrid time domain that, for each $j \in \mathbb{N}$, $t \mapsto \phi(t, j)$ is locally absolutely continuous on each interval $I^j := \{t : (t, j) \in \text{dom } \phi\}$ with nonempty interior.

The definition of a solution pair to a hybrid system is given as follows.

Definition 2.1 *Given a pair of functions $\phi : \text{dom } \phi \rightarrow \mathbb{R}^n$ and $u : \text{dom } u \rightarrow \mathbb{R}^m$, (ϕ, u) is a solution pair to (1) if $\text{dom}(\phi, u) := \text{dom } \phi = \text{dom } u$ is a hybrid time domain, $(\phi(0, 0), u(0, 0)) \in C \cup D$, and the following hold:*

- 1) *For all $j \in \mathbb{N}$ such that I^j has nonempty interior,*
 - a) *the function $t \mapsto \phi(t, j)$ is locally absolutely continuous over I^j ,*
 - b) *$(\phi(t, j), u(t, j)) \in C$ for all $t \in \text{int } I^j$,*
 - c) *the function $t \mapsto u(t, j)$ is Lebesgue measurable and locally bounded,*
 - d) *for almost all $t \in I^j$, $\dot{\phi}(t, j) = f(\phi(t, j), u(t, j))$.*
- 2) *For all $(t, j) \in \text{dom}(\phi, u)$ such that $(t, j+1) \in \text{dom}(\phi, u)$,*

$$(\phi(t, j), u(t, j)) \in D \quad \phi(t, j+1) = g(\phi(t, j), u(t, j))$$

Our motion planning algorithms require concatenating solution pairs. The concatenation operation of solution pairs is defined next.

Definition 2.2 *Given two functions $\phi_1 : \text{dom } \phi_1 \rightarrow \mathbb{R}^n$ and $\phi_2 : \text{dom } \phi_2 \rightarrow \mathbb{R}^n$, where $\text{dom } \phi_1$ and $\text{dom } \phi_2$ are hybrid time domains, ϕ_2 can be concatenated to ϕ_1 if ϕ_1 is compact and $\phi : \text{dom } \phi \rightarrow \mathbb{R}^n$ is the concatenation of ϕ_2 to ϕ_1 , denoted $\phi = \phi_1 | \phi_2$, namely:*

- 1) *$\text{dom } \phi = \text{dom } \phi_1 \cup (\text{dom } \phi_2 + \{(T, J)\})$, where $(T, J) = \max \text{dom } \phi_1$ and the plus sign denotes Minkowski addition;*
- 2) *$\phi(t, j) = \phi_1(t, j)$ for all $(t, j) \in \text{dom } \phi_1 \setminus \{(T, J)\}$ and $\phi(t, j) = \phi_2(t - T, j - J)$ for all $(t, j) \in \text{dom } \phi_2 + \{(T, J)\}$.*

2.3 C++ Notation

In this paper, the following C++ notation is used. Namespace is a declarative region providing scope to one or more identifiers. A lambda function is an anonymous function object that can be passed in as an argument. A pointer is a variable storage of the memory address of another variable. An asterisk *, when preceding a variable name at the time of declaration, is used to declare a pointer. The sequence of symbols :: is the scope resolution operator used to traverse scopes such as namespaces and classes, to access identifiers. A pair is a class coupling together two values that may have different types. Given two types T1 and T2, we write pairs in this paper as `std::pair<T1, T2>`. A double-valued scalar is a real, floating-point number with a maximum size of 64 bits.

The sequence of symbols \rightarrow is a member access operator used on pointers, to access members within the variable which has its memory address stored within the pointer. A data structure is a method of storing and organizing data within a program.

3 Motion Planning for Hybrid Dynamical Systems

This section formulates the motion planning problem for hybrid dynamical systems and introduces the data structure that implements the solution to this problem.

3.1 Problem Formulation

This paper solves a motion planning problem for hybrid dynamical systems, defined by flow and jump sets C and D , flow and jump maps f and g , along with the conditions to i) start from a given initial state, ii) end within a given goal state set, and iii) avoid reaching the unsafe set. This problem is mathematically formulated as follows.

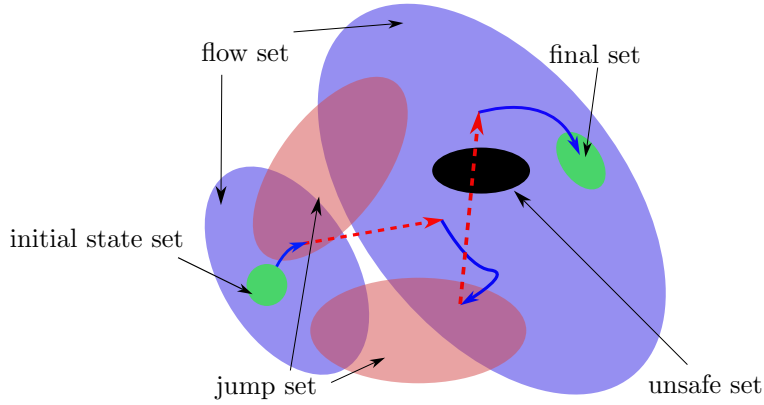


Figure 1: Illustration of a sample motion plan to problem 1, where the solid blue lines denote flow and dotted red lines denote jumps in the motion plan.

Problem 1 Given a hybrid system \mathcal{H} with input $u \in \mathbb{R}^m$ and state $x \in \mathbb{R}^n$, the initial state set $X_0 \subset \mathbb{R}^n$, the final state set $X_f \subset \mathbb{R}^n$, and the unsafe set $X_u \subset \mathbb{R}^n \times \mathbb{R}^m$, find a pair $(\phi, u) : \text{dom}(\phi, u) \rightarrow \mathbb{R}^n \times \mathbb{R}^m$, namely a motion plan as shown in Figure 1, such that for some $(T, J) \in \text{dom}(\phi, u)$, the following hold:

- 1) $\phi(0,0) \in X_0$, namely, the initial state of the solution belongs to the given initial state set X_0 ;
- 2) (ϕ, u) is a solution pair to \mathcal{H} as defined in Definition 2.1;
- 3) (T, J) is such that $\phi(T, J) \in X_f$, namely, the solution belongs to the final state set at hybrid time (T, J) ;
- 4) $(\phi(t, j), u(t, j)) \notin X_u$ for each $(t, j) \in \text{dom}(\phi, u)$ such that $t + j \leq T + J$, namely, the solution pair does not intersect with the unsafe set before its state trajectory reaches the final state set.

Therefore, given sets X_0 , X_f , and X_u , and a hybrid system \mathcal{H} with data (C, f, D, g) , a motion planning problem P is formulated as $P = (X_0, X_f, X_u, (C, f, D, g))$.

This problem is illustrated in the following example.

Example 3.1 (Actuated bouncing ball example) Consider the model of a bouncing ball where the ball is bouncing on a fixed horizontal surface. Following the model in Wang and Sanfelice [2022], the surface is located at the origin and, through control actions, is capable of affecting the velocity of the ball after the impact.

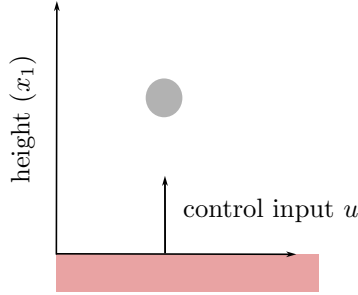


Figure 2: The actuated bouncing ball system.

The dynamics of the ball while in the air are given by

$$\dot{x} = \begin{bmatrix} x_2 \\ -\gamma \end{bmatrix} =: f(x, u) \quad (x, u) \in C$$

where $x := (x_1, x_2) \in \mathbb{R}^2$. The height of the ball is denoted by x_1 , as shown in Figure 2. The velocity of the ball is denoted by x_2 . The gravity constant is denoted by γ . The flow is allowed when the ball is on or above the surface. Hence, the flow set is $C := \{(x, u) \in \mathbb{R}^2 \times \mathbb{R} : x_1 \geq 0\}$. At every impact, the velocity of the ball changes from negative to positive while the height remains the same. The dynamics at jumps of the actuated bouncing ball system are given as

$$x^+ = \begin{bmatrix} x_1 \\ -\lambda x_2 + u \end{bmatrix} =: g(x, u) \quad (x, u) \in D$$

where $u \geq 0$ is the control input and $\lambda \in (0, 1)$ is the coefficient of restitution. Jumps are allowed when the ball is on the surface with nonpositive velocity. Hence, the jump set is $D := \{(x, u) \in \mathbb{R}^2 \times \mathbb{R} : x_1 = 0, x_2 \leq 0, u \geq 0\}$.

In a sample motion planning problem, the initial state set is defined as $X_0 = \{(1, 0)\}$, and the final state set as $X_f = \{(0, 0)\}$. In this problem, it is reasonable to assume that the input set has a lower and upper bound, and that those limits $u_{\min} \in \mathbb{R}$ and $u_{\max} \in \mathbb{R}$ should be real numbers satisfying $u_{\min} < u_{\max}$, which, in this example, are equal to 0 and 5, respectively. Therefore, the unsafe set is defined as $X_U = \{(x, u) \in \mathbb{R}^2 \times \mathbb{R} : u \in (-\infty, 0] \cup [5, \infty)\}$. The example motion planning problem is set as $P = (X_0, X_f, X_u, (C, f, D, g))$. Solutions to the bouncing ball system are presented later in this paper.

3.2 Data structures

Our motion planning algorithms search for motion plans by incrementally constructing search trees. The search tree is modeled by a directed tree. A directed tree \mathcal{T} is a pair $\mathcal{T} = (V, E)$, where V is a set whose elements are called vertices and E is a set of paired vertices whose elements are called edges. The edges in the directed tree are directed, which means the pairs of

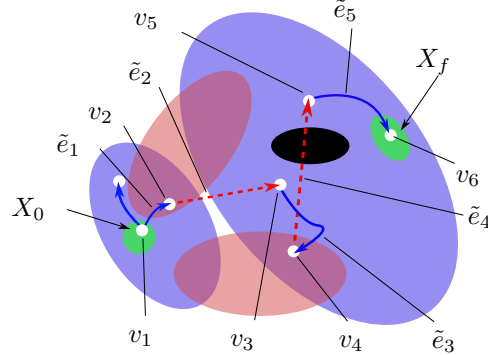


Figure 3: Illustration of the search tree constructed by HyRRT and HySST. The path $p = (v_1, v_2, \dots, v_6)$ and the solution pair $\tilde{e}_p = \tilde{e}_1|\tilde{e}_2|\dots|\tilde{e}_5$.

vertices that represent edges are ordered. The set of edges E is defined as $E \subseteq \{(v_1, v_2) : v_1 \in V, v_2 \in V, v_1 \neq v_2\}$. The edge $e = (v_1, v_2) \in E$ represents an edge from v_1 to v_2 . A path in $\mathcal{T} = (V, E)$ is a sequence of vertices $p = (v_1, v_2, \dots, v_k)$ such that $(v_i, v_{i+1}) \in E$ for each $i \in \{1, 2, \dots, k-1\}$.

Each vertex in the search tree \mathcal{T} is associated with a state value of \mathcal{H} . Each edge in the search tree is associated with a solution pair to \mathcal{H} that connects the state values associated with their endpoint vertices. The state value associated with vertex $v \in V$ is denoted as x_v and the solution pair associated with edge $e \in E$ is denoted as $\tilde{e} = (\phi, u)$, where $\phi : \text{dom } \phi \rightarrow \mathbb{R}^n, u : \text{dom } u \in \mathbb{R}^m$. The

solution pair that the path $p = (v_1, v_2, \dots, v_k)$ represents is the concatenation of all those solutions associated with the edges therein, namely,

$$\tilde{p} := \tilde{e}_{(v_1, v_2)} | \tilde{e}_{(v_2, v_3)} | \dots | \tilde{e}_{(v_{k-1}, v_k)}$$

where \tilde{p} denotes the solution pair associated with the path p .

3.2.1 State Space

As we assume the sets X_0, C, D, U_C , and U_D to have finite and positive Lebesgue measure [Wang and Sanfelice, 2024a, Assumption 6.15], we consider motion planning problems in a state space, which both algorithms make random selection from. To represent a state space of n dimension, constrained in each dimension by a minimum value `min_n` and a maximum value `max_n`, we first instantiate the state space as follows:

```
1 ompl::base::RealVectorStateSpace *statespace = new ompl::base::
  RealVectorStateSpace(0);
```

Then, we constrain each dimension by repeating the following with all n minimum and maximum values:

```
1 statespace->addDimension(min_n, max_n);
```

The dimension of the state space corresponds to the size of the state in the hybrid model. The order in which each dimension is added corresponds to its index when accessing states sampled from the state space. This is illustrated in the following example.

Example 3.2 (The actuated bouncing ball example in Example 3.1, revisited)

We instantiate the state space of the hybrid system in Example 3.1 as follows:

```
1 ompl::base::RealVectorStateSpace *statespace = new ompl::base::
  RealVectorStateSpace(0);
2 statespace->addDimension(min_1, max_1); // This is x_1 because it
  is added first
3 statespace->addDimension(min_2, max_2); // This is x_2 because it
  is added second
```

Then, when accessing states sampled from the state space, each dimension's order of addition corresponds to its index within the vector; for example, the first dimension to be added has a vector index of 0; the second dimension a vector index of 1, and so on.

```
1 // Assuming proper instantiation of ompl::base::State *state
2 double x_1 = state->as<ompl::base::RealVectorStateSpace::StateType
  >()->values[0];
3 double x_2 = state->as<ompl::base::RealVectorStateSpace::StateType
  >()->values[1];
```

Then, we implement the state value associated with vertex $v \in V$, x_v , as the OMPL class `ompl::base::State`², where a state is of n dimensions.

²See OMPL class reference: https://ompl.kavrakilab.org/classompl_1_1base_1_1State.html

3.2.2 Solution Pair

The vertex v is associated with a state value x_v and represents the endpoint of a solution pair \tilde{e} and edge e . Concatenation of solution pairs, as presented in Definition 2.2, is required by our motion planning algorithms, so we augment the OMPL data structure `Motion`³ to store an edge, which links the associated solution pair, inputs, and hybrid time to other objects of `Motion` which share either endpoint of edge e . The unmodified `Motion` class is as follows:

```

1  class Motion
2  {
3      public:
4          Motion() = default;
5          Motion(const base::SpaceInformationPtr &si) : state(si->
              allocState()){}
6
7          ~Motion() = default;
8          base::State *state{nullptr};
9          Motion *parent{nullptr};
10 };

```

The augmented `Motion` class is implemented as follows:

```

1  class Motion {
2      ompl::base::State *state{nullptr};
3      Motion *parent{nullptr};
4      std::vector<ompl::base::State *> *solutionPair{nullptr};
5      std::vector<std::pair<double, int>> hybridTime{nullptr};
6      std::vector<ompl::control::Control> inputs{nullptr};
7      // The following three attributes are only implemented in our
          second motion planning algorithm
8      unsigned numChildren_{0};
9      bool inactive_{false};
10     ompl::base::Cost accCost_{0.};
11 };

```

In the data structure `Motion`, the discretized solution pair \tilde{e} is implemented as a vector of states `solutionPair`, following the definition of a solution pair introduced in Section 2.1. The input associated with each discretized state, either sampled from U_C or U_D , is stored in `Motion` as a vector of control inputs `inputs`. Hybrid time associated with each discretized state is similarly stored as a vector in `Motion`, where (t, j) corresponds to `std::pair<double, int>` in line 5. All vectors are included as attributes of this `Motion` class, as their lengths are collectively dependent on the number of discretized steps. The complete implementation details for hybrid time, inputs, and edge associated with each `Motion` is introduced in the forthcoming subsections.

3.2.3 Hybrid Time

In the `Motion` datastructure, each state x is parameterized by a hybrid time (t, j) , where t is a double-valued scalar and j is an integer-valued scalar. Note that, as each state x must be parameterized by a hybrid time (t, j) , the number

³See: https://ompl.kavrakilab.org/classompl_1_1geometric_1_1RRT_1_1Motion.html

of state values generated by our motion planning algorithms must equal the number of hybrid times. Therefore, as this implementation depends on OMPL, which does not presently contain a state space class with the capability to capture hybrid time, we instead store the hybrid time as a vector of a pair with a double value and integer value, representing the flow time and number of jumps, respectively, for each state in the solution pair presented in Definition 3.2.2.

3.2.4 Inputs

In the **Motion** datastructure, the inputs are stored as vectors, associated with states in the discretized solution pair by vector. Input sets U_C and U_D have minimum and maximum values for each state, implemented as a 2-by- m arrays, containing double-valued scalars, where m denotes the dimension of input in (1).

3.2.5 Edge

In the **Motion** datastructure, the edge e is implemented as a C++ pointer to the left endpoint of the edge, or the **parent**. The right endpoint of the edge is represented by the vertex x_v , or **state**.

4 HyRRT Algorithm

Next, we introduce the main steps executed by HyRRT. Given the motion planning problem $P = (X_0, X_f, X_u, (C, f, D, g))$ and the input library (U_C, U_D) , HyRRT performs the following steps:

- Step 1: Sample a finite number of points from X_0 and initialize a search tree $\mathcal{T} = (V, E)$ by adding vertices associated with each sampling point.
- Step 2: Randomly select a point x_{rand} from C or D by randomly sampling from the state space and set checking using flow and jump sets C and D , respectively. The definite planning space is defined in Section 3.2.1.
- Step 3: Find the vertex v_{cur} associated with the state value that has minimal Euclidean distance to x_{rand} .
- Step 4: Randomly select an input signal (value) from U_C (U_D) if the flow (jump, respectively) regime is selected. Then, compute a solution pair using the flow map f or jump map g , starting from $x_{v_{\text{cur}}}$ with the selected input applied, denoted $\tilde{e}_{\text{new}} = (\phi_{\text{new}}, u_{\text{new}})$. If, during a simulation starting from the flow regime, ϕ_{new} intersects with the jump regime, compute an additional solution pair using the jump map from the collision vertex. Denote the final state of ϕ_{new} as x_{new} . If \tilde{e}_{new} does not intersect with X_u , add a vertex v_{new} associated with

x_{new} to V and an edge $(v_{\text{cur}}, v_{\text{new}})$ associated with \tilde{e}_{new} to E . Then, go to Step 2.

Following the above overview of HyRRT, the proposed algorithm is given in Algorithm 1. The inputs of Algorithm 1 are the problem $P = (X_0, X_f, X_u, (C, f, D, g))$, the input library (U_C, U_D) , a parameter $p_n \in (0, 1)$, which tunes the probability of proceeding with the flow regime or the jump regime, and an upper bound $K \in \mathbb{N}_{>0}$ for the number of iterations to execute, and two tunable sets $X_c \subset C$ and $X_d \subset D$, which act as constraints in finding a closest vertex to x_{rand} . Re-visiting the actuated bouncing ball example in Example 3.1, each function in Algorithm 1 is defined next.

4.1 $\mathcal{T} : \text{init}(X_0)$

The function call $\mathcal{T} : \text{init}$ is used to initialize a search tree $\mathcal{T} = (V, E)$. It randomly selects a finite number of points from X_0 . For each sampling point x_0 , a vertex v_0 associated with x_0 is added to V . At this step, no edge is added to E . The static function `initTree` implements this step, as shown below.

```

1 void ompl::geometric::HyRRT::initTree(void)
2 {
3     // get initial states with PlannerInputStates helper, pis_
4     while(const ompl::base::State *st = pis_.nextStart())
5     {
6         auto *motion = new Motion(si_);
7         si_>copyState(motion->state, st);
8         motion->root = motion->state;
9         // Add start motion to the tree object nn_
10        nn_>add(motion);
11    }
12 }
```

4.2 $x_{\text{rand}} \leftarrow \text{random_state}(S)$

The function call `random_state` randomly selects a point from the set $S \subseteq \mathbb{R}^n$. It is designed to select from C and D separately depending on the value of r rather than to select from $C \cup D$. The reason is that if C (or D) has zero measure while D (or C , respectively) does not, the probability that the point selected from $C \cup D$ lies in C (or D , respectively) is zero, which would prevent establishing probabilistic completeness. The flow and jump sets are defined as functions `flowSet_` and `jumpSet_`, respectively, and the random selection is implemented by the static function `randomSample`.

- 1) Jump set D is implemented as the lambda function `jumpSet_`. It takes in an arbitrary state as an input and outputs `true` if the state belongs to jump set D , and `false` if not. Below, we demonstrate how to implement the jump set for the actuated bouncing ball example.

```

1 bool jumpSet(Motion *v_cur) {
2     // The following implementation is used in the actuated
   bouncing ball example
```

```

3     double x2 = v_cur->state->as<ompl::base::
      RealVectorStateSpace::StateType>()->values[1];
4     double x1 = v_cur->state->as<ompl::base::
      RealVectorStateSpace::StateType>()->values[0];
5     double u = v_cur->inputs[0];
6
7     if (x1 <= 0 && x2 <= 0 && u >= 0)
8         return true;
9     else
10        return false;
11 }

```

- 2) Flow set C is implemented as the lambda function `flowSet_`. It takes in an arbitrary state as an input and outputs `true` if the state belongs to flow set C , and `false` if not. Below, we demonstrate how to implement the flow set for the actuated bouncing ball example.

```

1 bool flowSet(Motion *v_cur) {
2     return !jumpSet(v_cur);
3 }

```

- 3) `randomSample`: The OMPL `SpaceInformation` class's built-in state space sampler function is utilized to select a random state.

```

1 void ompl::geometric::HyRRT::randomSample(Motion *randomMotion
      )
2 {
3     ompl::base::StateSamplerPtr sampler_ = si_->
      allocStateSampler();
4     sampler_->sampleUniform(randomMotion->state);
5 }

```

4.3 $v_{\text{cur}} \leftarrow \text{nearest_neighbor}(x_{\text{rand}}, \mathcal{T}, H, \text{flag})$

The function call `nearest_neighbor` searches for a vertex v_{cur} in the search tree $\mathcal{T} = (V, E)$ such that its associated state value has minimal distance to x_{rand} . This function is implemented as follows.

- When `flag = flow`, the following optimization problem is solved over X_c :

Problem 2

$$\min_{v \in V} \|x_v - x_{\text{rand}}\| \quad s.t. \quad x_v \in X_c.$$

- When `flag = jump`, the following optimization problem is solved over X_d :

Problem 3

$$\min_{v \in V} \|x_v - x_{\text{rand}}\| \quad s.t. \quad x_v \in X_d.$$

The data of Problem 2 and Problem 3 comes from the arguments of the `nearest_neighbor` function call. This optimization problem can be solved by traversing all the

vertices in $\mathcal{T} = (V, E)$. The unsafe set is defined as the function `unsafeSet_`. Below, we present the static optimization function used to solve Problems 2 and 3, while demonstrating how to implement functions used to calculate the distance between two states and check for collision with the unsafe set, for the actuated bouncing ball example.

- 1) **setDistanceFunction**: Set the function that computes distance between states. Default-initialized to calculate Euclidean distance.

```

1 namespace ob = ompl::base;
2
3 double distanceFunction(ob::State *phi1, ob::State *phi2)
4 {
5     double dist = 0;
6     double x11 = (phi1->as<ob::RealVectorStateSpace::StateType
7 >())->values[0];
8     double x12 = (phi1->as<ob::RealVectorStateSpace::StateType
9 >())->values[1];
10    double x21 = (phi2->as<ob::RealVectorStateSpace::StateType
11 >())->values[0];
12    double x22 = (phi2->as<ob::RealVectorStateSpace::StateType
13 >())->values[1];
14    dist = sqrt(pow(x11 - x21, 2) + pow(x12 - x22, 2));
15    return fabs(dist);
16 }
17 cHyRRT.setDistanceFunction(distanceFunction);

```

- 2) **NearestNeighbors**: A built-in OMPL class is used to store and search within the search tree of `Motion` objects `nn_`, which is an object of `NearestNeighbors`. The function call `nearest` solves both Problem 2 and 3, returning the `Motion` in `nn_` with the lowest magnitude distance to the input `randomMotion`, according to the distance function set by `setDistanceFunction`.

```

1 std::shared_ptr<NearestNeighbors<Motion *>> nn_;
2 nn_->nearest(randomMotion);

```

- 3) The unsafe set X_u is implemented as the lambda function `unsafeSet_`. It takes in an arbitrary state as an input and outputs `true` if the state belongs to unsafe set X_u and `false` if not. Below, we demonstrate how to implement the unsafe set for the actuated bouncing ball example.

```

1 bool unsafeSet(Motion *motion) {
2     for(double u : motion->inputs){
3         if(u > 5 || u < 0)
4             return true;
5     }
6     return false;
7 }

```

4.4 `return` \leftarrow `new_state`($x_{\text{rand}}, v_{\text{cur}}, (U_C, U_D), H, X_u, x_{\text{new}}, \tilde{e}_{\text{new}}$)

If $x_{v_{\text{cur}}} \in C \setminus D$ (or $x_{v_{\text{cur}}} \in D \setminus C$), the function call `new_state` generates a new solution pair \tilde{e}_{new} to the hybrid system H starting from $x_{v_{\text{cur}}}$ by applying

an input signal \tilde{u} (or an input value u_D) randomly selected from U_C (or U_D , respectively). If $x_{v_{\text{cur}}} \in C \cap D$, then this function generates \tilde{e}_{new} by randomly selecting flows or jumps. The final state of \tilde{e}_{new} is denoted as x_{new} .

Note that the choices of inputs are random. After \tilde{e}_{new} and x_{new} are generated, the function `new_state` checks if there exists $(t, j) \in \text{dom}(\tilde{e}_{\text{new}})$ such that $\tilde{e}_{\text{new}}(t, j) \in X_u$. If so, then \tilde{e}_{new} intersects with the unsafe set, and `new_state` returns **false**. Otherwise, this function returns **true**. When $x_{v_{\text{cur}}} \in C$, `new_state` is implemented by the continuous simulator `continuousSimulator_`, and the solution pair is checked for collision with the jump regime using the function `collisionChecker_`. When $x_{v_{\text{cur}}} \in D$ or $x_{v_{\text{cur}}}$ experiences a collision with the jump regime during continuous propagation, `new_state` is implemented by the discrete simulator `discreteSimulator_`.

- 1) Flow map f is implemented within the lambda function `continuousSimulator_`⁴. While the state and input remains in the flow set C , the function uses numerical integration to propagate the state given the randomly generated flow time input. Each discretized integration step spans a duration specified by the user as class member variable `flowStepDuration_`. The control input u applied is randomly selected from control input set U_C . Next, we present the functions used to define the maximum propagation duration, discretized integration step duration, and control input set U_C :
 - a) `setTm`: Set the maximum flow time for a given flow propagation step. Value of `Tm_` must be positive.
 - b) `setFlowStepDuration`: Set the flow time for a given integration step, within a continuous simulation step. Value of `flowStepDuration_` must be positive and less than or equal to the maximum flow time `Tm_`.
 - c) `setFlowInputRange`: Set the vectors of minimum and maximum input values for integration in the flow regime. Minimum input values must be less than or equal to their corresponding maximum input values.

Below, we demonstrate how to implement and define the `continuousSimulator_` and its parameters using `setTm`, `setFlowStepDuration`, and `setFlowInputRange` for the actuated bouncing ball example.

```

1 namespace ob = ompl::base;
2
3 ob::State *continuousSimulator(std::vector<double> inputs, ob
  ::State *x_cur, double tFlow, ob::State *new_state) {
4     // Extract state values as a vector
5     auto *state_pointer = x_cur->as<ob::RealVectorStateSpace::
  StateType>();

```

⁴Following OMPL style for class member variables, we include an underscore after `continuousSimulator`. We treat `continuousSimulator_` as a member variable rather than a function because it is specific to instances of the class.

```

6     double x1 = state_pointer->values[0];
7     double x2 = state_pointer->values[1];
8     double x3 = state_pointer->values[2];
9
10    // Modify state values
11    new_state->values[0] = x1 + x2 * tFlow + (x3) * pow(tFlow,
12    2) / 2;
13    ...
14    return new_state;
15 }
16 ...
17 // See procedure to define state space in Section 3.1.1
18 ompl::base::RealVectorStateSpace *statespace = new ompl::base
19 ::RealVectorStateSpace(0);
20
21 // Construct a space information instance for this state space
22 ompl::base::StateSpacePtr space(statespace);
23 ompl::base::SpaceInformationPtr si(new ompl::base::
24 SpaceInformation(space));
25
26 si->setup();
27 ompl::geometric::HyRRT cHyRRT(si);
28 cHyRRT.setTm(0.5);
29 cHyRRT.setFlowInputRange(std::vector<double>{0}, std::vector<
30 double>{0});

```

The same approach to instantiating the tool on lines 20-24, where information defining the state space, contained in an instance of `RealVectorStateSpace`, is passed into an instance of `SpaceInformation`, and then into `HyRRT`, can be applied to both motion planning algorithms presented in this paper. The parameter definition method on line 25 can be generalized toward the remaining customizable parameters, by replacing `Tm` with the name of the parameter, with the exception of the control input ranges. The method used to define U_C on line 26 can be generalized to U_D , by replacing `setFlowInputRange` with `setJumpInputRange`.

- 2) Jump map g is implemented within the lambda function `discreteSimulator_`. The function `discreteSimulator_` returns a state propagated once. The control input is defined as $u \in U_D$. Below, we demonstrate how to implement the `discreteSimulator_` for the actuated bouncing ball example.

```

1     namespace ob = ompl::base;
2
3     ob::State *discreteSimulator(std::function<ob::State *(ob::
4     State *curState, std::vector<double> u, ob::State *
5     newState)) {
6         double x2 = -0.8 * x_cur->as<ompl::base::
7         RealVectorStateSpace::StateType>()->values[1];
8         ...
9         new_state->as<ompl::base::RealVectorStateSpace::StateType
10         >()->values[1] = x2 - u[0];
11         ...
12         return new_state;

```


11 }

Next, we present the function used to define the control input set U_D :

setJumpInputRange: Set the vectors of minimum and maximum input values for integration in the jump regime. Minimum values must be less than or equal to their corresponding maximum values. Below, we demonstrate how to define the jump input range for the actuated bouncing ball example.

```
1 cHyRRT.setJumpInputRange(std::vector<double>{0}, std::vector<double>{5});
```

- 3) The collision checker is implemented as the lambda function **collisionChecker_**. It takes in an input of an edge and, if a collision occurs, outputs **true** and updates the edge right endpoint to reflect the collision state. If no collision occurs, then the function outputs **false** and makes no modification to the edge. By default, the function is a point-by-point collision checker that checks each point using the **jumpSet_**. Below, we demonstrate how to implement the collision checker for a general motion planning problem, as the actuated bouncing ball example uses the default, point-by-point collision checker and therefore does not define a new collision checker.

```
1 namespace ob = ompl::base;
2
3 bool collisionChecker(std::vector<ob::State*> *solutionPair,
4   std::function<bool(ob::State *state)> obstacleSet, double
5   ts, double tf, ob::State *new_state, int tFIndex) {
6   // Modify state if needed
7   ...
8   return false;
9 }
```

4.5 $v_{\text{new}} \leftarrow \mathcal{T} : \text{add_vertex}(x_{\text{new}})$ and $\mathcal{T} : \text{add_edge}(v_{\text{cur}}, v_{\text{new}}, \tilde{e}_{\text{new}})$

The function call $\mathcal{T} : \text{add_vertex}(x_{\text{new}})$ adds a new vertex v_{new} associated with x_{new} to \mathcal{T} and returns v_{new} . The function call $\mathcal{T} : \text{add_edge}(v_{\text{cur}}, v_{\text{new}}, \tilde{e}_{\text{new}})$ adds a new edge $e_{\text{new}} = (v_{\text{cur}}, v_{\text{new}})$ associated with \tilde{e}_{new} to \mathcal{T} . A solution checking function is employed to check if a path in \mathcal{T} can be used to construct a motion plan to the given motion planning problem. If this function finds a path $p = ((v_0, v_1), (v_1, v_2), \dots, (v_{n-1}, v_n)) =: (e_0, e_1, \dots, e_{n-1})$ in \mathcal{T} such that 1) $x_{v_0} \in X_0$ and 2) $x_{v_n} \in X_f$, then the solution pair \tilde{e}_p is a motion plan to the given motion planning problem. In practice, item 2 is too restrictive. Given $\epsilon > 0$ representing the tolerance with this condition, we implement item 2 as $\text{dist}(x_{v_n}, X_f) \leq \epsilon$, with the following function **setGoalTolerance**.

- 1) **setGoalTolerance**: Set the distance tolerance from the goal state for a state to be recognized as a valid final state. Default-initialized to be 0.1. Must be greater than or equal to zero.

```

1 double goalTolerance = ...;
2 cHyRRT.setGoalTolerance(goalTolerance);

```

Algorithm 1 HyRRT algorithm

Input: $X_0, X_f, X_u, \mathcal{H} = (C, f, D, g), (U_C, U_D), p \in (0, 1), K \in \mathbb{N} > 0$

```

1:  $\mathcal{T} \leftarrow \text{init}(X_0)$ 
2: for  $k = 1$  to  $K$  do
3:   randomly select a real number  $r$  from  $[0, 1]$ 
4:   if  $r \leq p$  then
5:      $x_{\text{rand}} \leftarrow \text{random\_state}(C)$ 
6:      $\text{extend}(\mathcal{T}, x_{\text{rand}}, (U_C, U_D), \mathcal{H}, X_u, \text{flow})$ 
7:   else
8:      $x_{\text{rand}} \leftarrow \text{random\_state}(D)$ 
9:      $\text{extend}(\mathcal{T}, x_{\text{rand}}, (U_C, U_D), \mathcal{H}, X_u, \text{jump})$ 
10:  end if
11: end for
12: return  $\mathcal{T}$ 

1: function  $\text{extend}(\mathcal{T}, x, (U_C, U_D), \mathcal{H}, X_u, \text{flag})$ 
2:  $v_{\text{cur}} \leftarrow \text{nearest\_neighbor}(x, \mathcal{T}, \mathcal{H}, \text{flag})$ 
3: if new state( $x, v_{\text{cur}}, (U_C, U_D), \mathcal{H}, X_u, x_{\text{new}}, \tilde{e}_{\text{new}}$ ) then
4:    $v_{\text{new}} \leftarrow \mathcal{T}.\text{add\_vertex}(x_{\text{new}})$ 
5:    $\mathcal{T}.\text{add\_edge}(v_{\text{cur}}, v_{\text{new}}, \tilde{e}_{\text{new}})$ 
6:   if  $x_{\text{new}} == x$  then
7:     return Reached
8:   else
9:     return Advanced
10:  end if
11: end if
12: return Trapped

```

4.6 Post-processing Scripts

The post-processing script detailed below is followed by an example implementation.

- 1) **roslaunch**: Script to visualize the trajectory using data located in `$rootDirectory/examples/visualize/points.txt` in ROS 2's RViz 2. Visualization is limited to 2-3 dimensions. Follow command-line interface directives to assign data columns to dimensions.

```

1 ./roslaunch.bash

```

5 HySST Algorithm

HySST generates asymptotically near-optimal solutions, with only two notable deviations from the main steps of HyRRT, as outlined in Section 4:

Algorithm 2 HySST algorithm

Input: $X_0, X_f, X_u, \mathcal{H} = (C, f, D, g), (U_C, U_D), p_n \in (0, 1), K \in \mathbb{N}_{>0}, X_c, X_d, \epsilon_{BN}, \epsilon_s$

```

1:  $\mathcal{T} \leftarrow \text{init}(X_0)$ 
2:  $V_{\text{active}} \leftarrow V, V_{\text{inactive}} \leftarrow \emptyset, S \leftarrow \emptyset$ 
3: for all  $v_0 \in V$  do
4:   if is_vertex_locally_the_best( $x_{v_0}, 0, S, \epsilon_s$ ) then
5:      $(S, V_{\text{active}}, V_{\text{inactive}}, E) \leftarrow \text{prune\_dominated\_vertices}(v_0, S, V_{\text{active}}, V_{\text{inactive}}, E)$ 
6:   end if
7: end for
8: for  $k = 1$  to  $K$  do
9:   randomly select a real number  $r$  from  $[0, 1]$ 
10:  if  $r \leq p_n$  then
11:     $x_{\text{rand}} \leftarrow \text{random\_state}(C)$ 
12:     $v_{\text{cur}} \leftarrow \text{best\_near\_selection}(x_{\text{rand}}, V_{\text{active}}, \epsilon_{BN}, X_c)$ 
13:  else
14:     $x_{\text{rand}} \leftarrow \text{random\_state}(D)$ 
15:     $v_{\text{cur}} \leftarrow \text{best\_near\_selection}(x_{\text{rand}}, V_{\text{active}}, \epsilon_{BN}, X_d)$ 
16:  end if
17:   $(\text{is\_a\_new\_vertex\_generated}, x_{\text{new}}, \tilde{e}_{\text{new}}, \text{cost}_{\text{new}}) \leftarrow \text{new\_state}(v_{\text{cur}}, (U_C, U_D), \mathcal{H}, X_u)$ 
18:  if is\_a\_new\_vertex\_generated and is\_vertex\_locally\_the\_best( $x_{\text{new}}, \text{cost}_{\text{new}}, S, \epsilon_s$ ) then
19:     $v_{\text{new}} \leftarrow V_{\text{active}}.\text{add\_vertex}(x_{\text{new}}, \text{cost}_{\text{new}})$ 
20:     $E.\text{add\_edge}(v_{\text{cur}}, v_{\text{new}}, \tilde{e}_{\text{new}})$ 
21:     $(S, V_{\text{active}}, V_{\text{inactive}}, E) \leftarrow \text{prune\_dominated\_vertices}(v_{\text{new}}, S, V_{\text{active}}, V_{\text{inactive}}, E)$ 
22:  end if
23: end for
24: return  $\mathcal{T}$ 

```

Step 3: Find the vertex v_{cur} associated with the state value that has the minimal cost functional, within the neighborhood defined by a ball of radius ϵ_{BN} of x_{rand} . If no vertex exists within the neighborhood, the nearest vertex in V is selected. Below, we demonstrate how to set the selection radius ϵ_{BN} .

- 1) **setSelectionRadius**: Set the scalar value ϵ_{BN} used to select vertex closest to the randomly sampled vertex. Must be greater than or equal to zero.

```

1 double selectionRadius = ...;
2 cHySST.setSelectionRadius(selectionRadius);

```

Step 4: Once a solution pair is computed as outlined in Section 4, if \tilde{e}_{new} does not intersect with X_u and v_{new} has a minimal cost within the neighborhood defined by a ball of radius ϵ_S , add the vertex v_{new} associated with x_{new} to V and an edge $(v_{\text{cur}}, v_{\text{new}})$ associated with \tilde{e}_{new} to E . Then, the pruning process removes from the search tree the vertices with higher cost in the neighborhood of the new vertex defined by a ball of radius ϵ_S . This additional step maintains a static set of witnesses to sparsify the vertices. Below, we demonstrate how to define the pruning radius ϵ_S .

setPruningRadius: Set the scalar value ϵ_S used to surround and remove representative vertices of the witness set. Must be either zero or positive.

```

1 double pruningRadius = ...;
2 cHySST.setPruningRadius(pruningRadius);

```

5.1 Initialization Functions

The initialization function detailed below is followed by an example implementation.

setBatchSize: Set the number of solutions allowed in one instance of HySST. Once the maximum number of solutions is reached, the tool's **solve** function, which generates the solution path, will return the solution with the lowest cost. Default-initialized to be 1. Must be a positive integer.

```

1 double batchSize = ...;
2 cHyRRT.setBatchSize(batchSize);

```

6 Examples

Next, we illustrate both cHyRRT and cHySST in two hybrid systems modeled as hybrid equations.⁵

6.1 Bouncing Ball (revisited)

The following procedure is used to generate a solution to the motion planning problem for the specific instance of the bouncing ball system presented in Example 3.1 using cHyRRT:

⁵The files associated with the two examples are available at the software entry at <https://github.com/HybridSystemsLab/hybridRRT-Ccode/README.md> and <https://github.com/HybridSystemsLab/hybridSST-Ccode/README.md>.

- 1) Inside the C++ file `bouncing_ball.cpp`, initial state, final state, and unsafe sets are defined, along with a step size coefficient of 0.001, a gravity constant γ of 9.81, a goal tolerance of 0.1, flow input range $U_C = \{0, 0\}$, and jump input range $U_D = \{0, 5\}$.
- 2) Then, the functions `flowSet_`, `jumpSet_`, `continuousSimulator_`, and `discreteSimulator_` are implemented according to the flow and jump sets C and D and flow and jump maps f and g as illustrated in Example 3.1.
- 3) Finally, the motion planner is run using the `solve` function within cHyRRT to return a trajectory.

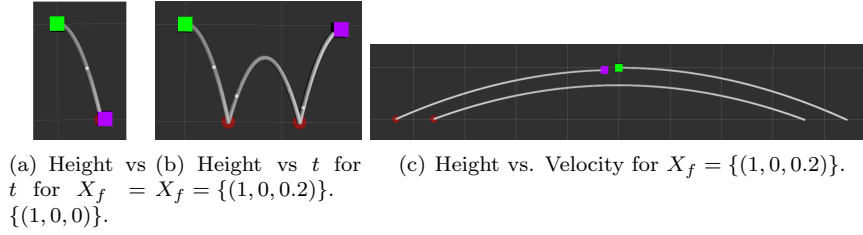


Figure 4: Simulated solutions to actuated bouncing ball example in Section 3.1. The start and goal vertices are marked by green and purple squares, respectively, and vertices in the jump regime are marked by red circles.

A simulated solution to the bouncing ball system is depicted using a graph of the ball's height vs. time in Figure 4a. In addition, for an instance of the problem where $X_f = \{(1, 0, 0.2)\}$, a graph of the ball's height over time and the ball's height over its velocity are shown in Figure 4b and 4c, respectively.

6.2 Collision-resilient Tensegrity Multicopter

A simulated solution to a collision-resilient tensegrity multicopter in the horizontal plane that can operate after colliding with a concrete wall is shown, where the position of the multicopter along the y -axis of the ball is plotted as a function of the position along the x -axis.

As previously defined in Wang and Sanfelice [2023], the state of the multicopter is composed of the position vector $p := (p_x, p_y) \in \mathbb{R}^2$, where p_x denotes the position along the x -axis and p_y denotes the position along the y -axis, the velocity vector $v := (v_x, v_y) \in \mathbb{R}^2$, where v_x denotes the velocity along the x -axis and v_y denotes the velocity along the y -axis, and the acceleration vector $a := (a_x, a_y) \in \mathbb{R}^2$ where a_x denotes the acceleration along the x -axis and a_y denotes the acceleration along the y -axis. The state of the system is $x := (p, v, a) \in \mathbb{R}^6$ and its input is $u := (u_x, u_y) \in \mathbb{R}^2$. The environment is assumed to be known. Define the region of the walls as $W \subset \mathbb{R}^2$, represented by white rectangles in Figure 5.

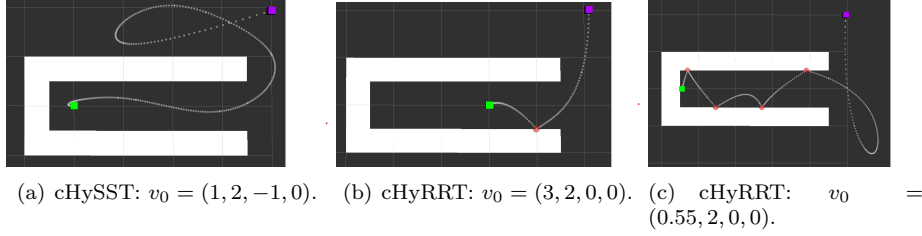


Figure 5: Simulated solution to the multicopter example, graphed as x_1 vs x_2 . The start and goal vertices are marked by green and purple squares, respectively, and vertices in the jump regime are marked by red circles.

Flow is allowed when the multicopter is in the free space. Hence, the flow set is $C := \{((p, v, a), u) \in \mathbb{R}^6 \times \mathbb{R}^2 : p \notin W\}$. The dynamics of the quadrotors when no collision occurs can be captured using time-parameterized polynomial trajectories because of its differential flatness as Liu et al. [2017]

$$\dot{x} = \begin{bmatrix} v \\ a \\ u \end{bmatrix} =: f(x, u) \quad (x, u) \in C.$$

Note that the post-collision position stays the same as the pre-collision position. Therefore, $p^+ = p$. Denote the velocity component of $v = (v_x, v_y)$ that is normal to the wall as v_n and the velocity component that is tangential to the wall as v_t . Then, the velocity component v_n after the jump is modeled as $v_n^+ = -e v_n =: g_{v_n}(v)$ where $e \in (0, 1)$ is the coefficient of restitution. The velocity component v_t after the jump is modeled as $v_t^+ = v_t + \kappa(-e - 1) \arctan\left(\frac{v_t}{v_n}\right) =: g_{v_t}(v)$ where $\kappa \in \mathbb{R}$ is a constant; see [14]. Denote the projection of the updated vector (v_n^+, v_t^+) onto the x -axis as $\bar{x}(v_n^+, v_t^+)$ and the projection of the updated vector (v_n^+, v_t^+) onto the y -axis as $\bar{y}(v_n^+, v_t^+)$. Therefore,

$$v^+ = \begin{bmatrix} \bar{x}(g_{v_n}(v), g_{v_t}(v)) \\ \bar{y}(g_{v_n}(v), g_{v_t}(v)) \end{bmatrix} =: g_v(v).$$

We assume that $a^+ = 0$. The discrete dynamics capturing the collision process is modeled as

$$x^+ = \begin{bmatrix} p \\ g_v(v) \\ 0 \end{bmatrix} =: g(x, u) \quad (x, u) \in D.$$

The jump is allowed when the multicopter is on the wall surface with positive velocity towards the wall. Hence, the jump set is

$$D := \{((p, v, a), u) \in \mathbb{R}^6 \times \mathbb{R}^2 : p \in \partial W, v_n < 0\}.$$

Given the initial state set as $X_0 = \{(1, 2, 0, 0, 0, 0)\}$, the final state set as $X_f = \{(5, 4)\} \times \mathbb{R}^4$, and the unsafe set as

$$X_u = \{(x, u) \in \mathbb{R}^6 \times \mathbb{R}^2 : p_x \in (-\infty, 0] \cup [6, \infty), \\ p_y \in (-\infty, 0] \cup [5, \infty), (p_x, p_y) \in \text{int } W\}, \quad (2)$$

the following procedure is used to generate a solution to the motion planning problem for this system using cHySST: 1) Inside the C++ file `multicopter.cpp`, initial conditions, a step size coefficient, optimization objective, and input ranges are defined; 2) Then, the functions `flowSet_`, `jumpSet_`, `unsafeSet_`, `continuousSimulator_`, and `discreteSimulator_` are edited according to the data given above; 3) Finally, the motion planner is run using `solve` function within cHySST to return a trajectory. A simulated solution to the collision-resilient drone system is depicted using a graph of the drone's y position over its x position in Figure 5.

6.2.1 Evolution of Solution Costs Over Range of HySST Solution Batch Sizes

From data collected over 10 runs of HySST solving the collision-resilient drone motion planning problem, the minimum and mean cost of all 10 lowest-cost solutions, within solutions batches of increasing size, displays an inverse correlation between solution batch size and the cost of the lowest-cost solution.

However, while increasing batch size generally reduces the cost of the generated solution with the best cost, it also increases computational consumption. As more of the planning space is explored and vertices are sparsified, the rate at which new vertices v_{new} are added to V declines, increasing the difficulty of finding a unique, lower-cost solution.

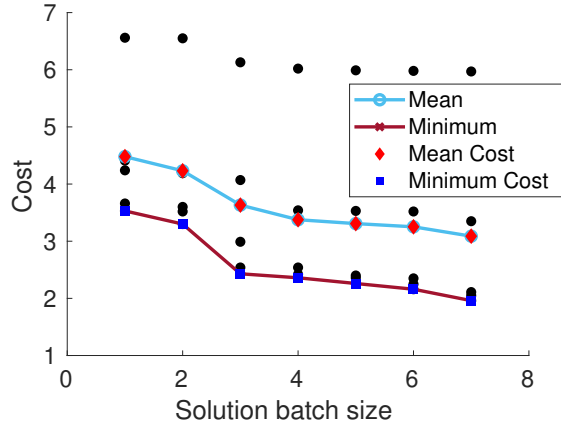


Figure 6: Cost of lowest-cost solution given a solution batch size.

7 Conclusion

The two tools cHyRRT and cHySST for planning of hybrid systems was described and illustrated in examples. Leveraging the computational efficiency of C++, applicability to high-dimensional, hybrid systems of the RRT-type and SST-type tools, and generalizability of OMPL and ROS to robotics applications, we present two highly versatile motion planning tools. cHyRRT can be installed from <https://github.com/HybridSystemsLab/hybridRRT-Ccode> and cHySST from <https://github.com/HybridSystemsLab/hybridSST-Ccode>.

In future work, we will implement HyRRT-Connect, a bidirectional RRT algorithm presented in Wang and Sanfelice [2024b], in C++/OMPL.

References

- Nan Wang and Ricardo G Sanfelice. A rapidly-exploring random trees motion planning algorithm for hybrid dynamical systems. In *2022 IEEE 61st Conference on Decision and Control (CDC)*, pages 2626–2631. IEEE, 2022.
- Nan Wang and Ricardo G. Sanfelice. Hysst: An asymptotically near-optimal motion planning algorithm for hybrid systems. In *2023 62nd IEEE Conference on Decision and Control (CDC)*, pages 2865–2870, 2023. doi: 10.1109/CDC49753.2023.10383466.
- Ana Lopes, Joao Rodrigues, Jorge Perdigao, Gabriel Pires, and Urbano Nunes. A new hybrid motion planner: Applied in a brain-actuated robotic wheelchair. *IEEE Robotics & Automation Magazine*, PP:1–1, 11 2016. doi: 10.1109/MRA.2016.2605403.
- Lei Yang, Chao Lu, Guangming Xiong, Yang Xing, and Jianwei Gong. A hybrid motion planning framework for autonomous driving in mixed traffic flow. *Green Energy and Intelligent Transportation*, 1(3):100022, 2022. ISSN 2773-1537. doi: <https://doi.org/10.1016/j.geits.2022.100022>. URL <https://www.sciencedirect.com/science/article/pii/S2773153722000226>.
- Priyaranjan Biswal and Prases K. Mohanty. Development of quadruped walking robots: A review. *Ain Shams Engineering Journal*, 12(2):2017–2031, 2021. doi: <https://doi.org/10.1016/j.asej.2020.11.005>. URL <https://www.sciencedirect.com/science/article/pii/S2090447920302501>.
- C. Piazza, G. Grioli, M.G. Catalano, and A. Bicchi. A century of robotic hands. *Annual Review of Control, Robotics, and Autonomous Systems*, 2 (Volume 2, 2019):1–32, 2019. ISSN 2573-5144. doi: <https://doi.org/10.1146/annurev-control-060117-105003>. URL <https://www.annualreviews.org/content/journals/10.1146/annurev-control-060117-105003>.
- Faiyaz Ahmed, J. C. Mohanta, Anupam Keshari, and Pankaj Singh Yadav. Recent advances in unmanned aerial vehicles: A review. *Arabian Jour-*

- nal for Science and Engineering*, 47(7):7963–7984, Apr 2022. doi: 10.1007/s13369-022-06738-0.
- Ioan A. Şucan, Mark Moll, and Lydia E. Kavraki. The Open Motion Planning Library. *IEEE Robotics & Automation Magazine*, 19(4):72–82, 12 2012. doi: 10.1109/MRA.2012.2205651. <https://ompl.kavrakilab.org>.
- Marlin P. Strub and Jonathan D. Gammell. Advanced bit* (abit*): Sampling-based planning with advanced graph-search techniques. In *2020 IEEE International Conference on Robotics and Automation (ICRA)*, pages 130–136, 2020. doi: 10.1109/ICRA40945.2020.9196580.
- Francesco Grothe, Valentin N. Hartmann, Andreas Orthey, and Marc Toussaint. St-rrt*: Asymptotically-optimal bidirectional motion planning through space-time. In *Proc. of the IEEE Int. Conf. on Robotics and Automation (ICRA)*, 2022.
- Ryan Luna, Mark Moll, Julia Badger, and Lydia E Kavraki. A scalable motion planner for high-dimensional kinematic systems. *The International Journal of Robotics Research*, 39(4):361–388, 2020. doi: 10.1177/0278364919890408. URL <https://doi.org/10.1177/0278364919890408>.
- Rafal Goebel, Ricardo G Sanfelice, and Andrew R Teel. Hybrid dynamical systems. *IEEE Control Systems Magazine*, 29(2):28–93, 2009.
- Michael S Branicky, Michael M Curtiss, John Levine, and Scott Morgan. Sampling-based planning and control. In *Proceedings of the 12th Yale Workshop on Adaptive and Learning Systems*, New Haven, CT, 2003. Citeseer.
- Steven M. LaValle. Rapidly-exploring random trees : a new tool for path planning. *The annual research report*, 1998. URL <https://api.semanticscholar.org/CorpusID:14744621>.
- Yajue Yang. Survey of optimal motion planning. *IET Cyber-Systems and Robotics*, 1:13–19(6), 6 2019. URL <https://digital-library.theiet.org/content/journals/10.1049/iet-csr.2018.0003>.
- Oren Nechushtan, Barak Raveh, and Dan Halperin. Sampling-diagram automata: A tool for analyzing path quality in tree planners. volume 68, pages 285–301, 01 2010. ISBN 978-3-642-17451-3. doi: 10.1007/978-3-642-17452-0_17.
- Sertac Karaman and Emilio Frazzoli. Sampling-based algorithms for optimal motion planning. *The International Journal of Robotics Research*, 30(7):846–894, 2011. doi: 10.1177/0278364911406761. URL <https://doi.org/10.1177/0278364911406761>.
- Yanbo Li, Zakary Littlefield, and Kostas E. Bekris. Asymptotically optimal sampling-based kinodynamic planning. *The International Journal of Robotics Research*, 35(5):528–564, 2016. doi: 10.1177/0278364915614386. URL <https://doi.org/10.1177/0278364915614386>.

- Steven Macenski, Tully Foote, Brian Gerkey, Chris Lalancette, and William Woodall. Robot operating system 2: Design, architecture, and uses in the wild. *Science Robotics*, 7(66):eabm6074, 2022. doi: 10.1126/scirobotics.abm6074. URL <https://www.science.org/doi/abs/10.1126/scirobotics.abm6074>.
- Nan Wang and Ricardo G. Sanfelice. Motion planning for hybrid dynamical systems: Framework, algorithm template, and a sampling-based approach, 2024a. URL <https://arxiv.org/abs/2406.01802>.
- Sikang Liu, Nikolay Atanasov, Kartik Mohta, and Vijay Kumar. Search-based motion planning for quadrotors using linear quadratic minimum time control. In *2017 IEEE/RSJ International Conference on Intelligent Robots and Systems (IROS)*, pages 2872–2879, 2017. doi: 10.1109/IROS.2017.8206119.
- Nan Wang and Ricardo G. Sanfelice. Hyrrt-connect: A bidirectional rapidly-exploring random trees motion planning algorithm for hybrid systems, 2024b. URL <https://arxiv.org/abs/2403.18413>.